Journal of Thermal Analysis and Calorimetry, Vol. 92 (2008) 1, 7–13

THERMAL BEHAVIOUR STUDY OF SOME SOL–GEL TiO_2 BASED MATERIALS

Maria Crişan[1*], *Ana Brăileanu*[1], *D. Crişan*[1], *Mălina Răileanu*[1], *N. Drăgan*[1], *Diana Mardare*[2], *V. Teodorescu*[3], *Adelina Ianculescu*[4], *Ruxandra Bîrjega*[5] *and M. Dumitru*[5]

[1]Institute of Physical Chemistry 'Ilie Murgulescu', Laboratory of Oxide Materials Science, 202 Splaiul Independenţei 060021 Bucharest, Romania
[2]'Al.I. Cuza' University, Faculty of Physics, 11 Carol I Blvd., 700506 Iaşi, Romania
[3]National Institute for Physics of Materials, P.O. Box MG 07, Bucharest, Măgurele, Romania
[4]University 'Politehnica', 1 Gh. Polizu, 011061, Bucharest, Romania
[5]National Institute for Lasers, Plasma and Radiation Physics, P.O. Box MG-36, 769000 Bucharest, Romania

Among the great number of sol–gel materials prepared, TiO_2 holds one of the most important places due to its photocatalytic properties, both in the case of powders and coatings. Impurity doping is one of the typical approaches to extend the spectral response of a wide band gap semiconductor to visible light.

This work has studied some un-doped and Pd-doped sol–gel TiO_2 nanopowders, presenting various surface morphologies and structures. The obtained powders have been embedded in vitreous TiO_2 matrices and the corresponding coatings have been prepared by dipping procedure, on glass substrates. The relationship between the synthesis conditions and the properties of titania nanosized materials, such as thermal stability, phase composition, crystallinity, morphology and size of particles, and the influence of dopant was investigated.

The influence of Pd on TiO_2 crystallization both for supported and unsupported materials was studied (lattice parameters, crystallite sizes, internal strains). The hydrophilic properties of the films were also connected with their structure, composition and surface morphology. The methods used for the characterization of the materials have been: simultaneous thermogravimetry and differential thermal analysis, powder X-ray diffraction, electron microscopy (TEM, SAED) and AFM.

Keywords: *films from nanopowders, hydrophilicity, nanopowders, Pd-doped TiO_2 materials, sol–gel process, thermal behaviour, un-doped TiO_2 materials*

Introduction

Nanostructured titania has been reported to be used in many applications in areas ranging from optics via solar energy to gas sensors. Among the great number of sol–gel materials prepared, TiO_2 holds one of the most important places due to its photocatalytic properties, both in the case of powders and coatings. The preferential use of TiO_2 in the photocatalytic degradation of organic pollutants is based on its high oxidative power, photostability and nontoxicity [1–4]. It can be considered as one of the new Advanced Oxidation Technologies (AOT) for air and water treatment. Recently, Wang *et al*. and Miyauchi *et al*. reported another new application of TiO_2 in photochemistry, self-cleaning and antifogging based on the photoinduced hydrophilicity [5, 6]. Because chemical reactions take place only on the surface of a catalyst, the surface modifications can greatly affect the adsorption of all reactants and reaction efficiency. The photoinduced hydrophilicity, photocatalytic H_2 evolution and organic contaminant decomposition are greatly improved by the insertion of fluorine [7]; it increases the surface acidity of TiO_2 because of the strongest electronegativity of fluorine.

However, one disadvantage of this semiconductor material is the large band-gap, 3.2 eV for bulk TiO_2, which limits the photosensitivity to the UV region. Impurity doping is one of the typical approaches to extend the spectral response of a wide band gap semiconductor to visible light. The 3d-transitional metal doped anatase TiO_2 is the usual modification method [8]. These metals loading can decrease the recombination of photogenerated holes and electrons and promote interfacial electron transfer. There are many papers dealing with the sol–gel preparation of TiO_2 anatase with tailored morphological features and some of them review the thermal behaviour of the TiO_2 gels by other investigations [9–14]. There are only few literature data regarding the use of Pd as cation dopant in a sol–gel TiO_2 matrix [15, 16].

Conventional TiO_2 powder catalysts present the disadvantages of agglomeration and of the difficult separation of the final particle-fluid for the catalyst

* Author for correspondence: mcrisan@icf.ro

1388–6150/$20.00

Akadémiai Kiadó, Budapest, Hungary
Springer, Dordrecht, The Netherlands

recycling. Thus, the application of the TiO_2 thin films has attracted much attention in the last years. Our previous work [17] presents the results on processing and structural and optical characteristics of un-doped and Pd-doped sol–gel TiO_2 coatings, obtained in situ, by co-gelation of both components in solution.

A novel method for the processing of sol–gel derived titanium dioxide composites as thick film coatings and self-supported bulk species has been developed by Kesmiri *et al*. [18]. The composite sol–gel coatings showed photocatalytic activities comparable with the powder Degussa (P-25) titania photocatalyst.

The present work has studied some un-doped and Pd-doped sol–gel TiO_2 nanopowders, obtained by simultaneous gelation of both precursors $Ti(OEt)_4$ and $Pd(acac)_2$, presenting various surface morphologies and structures. The obtained materials have been embedded in vitreous TiO_2 matrices and un-doped and Pd-doped TiO_2 coatings have been prepared by dipping procedure using glass substrates. The hydrophilic properties of the films were connected with their structure, composition and surface morphology.

Experimental

TiO_2 based sol–gel nanopowders preparation

In order to obtain un-doped and Pd-doped TiO_2 films from sol–gel nanopowders, the first goal of the work was to prepare the powders. Both pure and 1% Pd containing TiO_2 powders have been synthesized using the alkoxide route of the sol–gel method. In all cases the tetraethylorthotitanate (Merck), $Ti(OC_2H_5)_4$ represented the TiO_2 source. For the doped samples the source of Pd was Pd acetylacetonate (Merck), $Pd(acac)_2$. As solvent for both mentioned precursors the absolute ethanol (Riedel de Haën) was used. The hydrolysis of titanium alkoxide took place with a water excess. Details concerning the sol–gel TiO_2 nanopowders preparation are presented in one of our recent works [19]. The obtained powders have been dried at 80°C and then thermally treated at 300, 400, and 500°C for 1 h, according to DTA/TG results.

TiO_2 matrix preparation

In all cases, the used matrix consisted from a sol of pure TiO_2 obtained from the same TiO_2 alkoxide precursor as in the case of powders, tetraethylorthotitanate (Merck) $Ti(OC_2H_5)_4$, respectively. The solvent of the Ti alkoxide was absolute ethanol (Riedel de Haën) and the hydrolysis reaction took place in the presence of the water, added in substoichiometric quantity. The hydrolysis reaction was carried out in a closed system in nitrogen atmosphere under vigorous stirring. A very rigorous pH and viscosity control of the TiO_2 sol was necessary in order to establish the most propitious moment for including the sol-gel prepared nanopowders. This was possible based on previous systematic studies and on the sol-gel experience of our team [17]. The nitric acid was used as catalyst to obtain a final pH of the sol of ~4. In order to compare the structural behaviour of the nanopowders and of the TiO_2 matrix with the thermal processing, the same thermal schedules have been applied.

Un-doped and Pd-doped TiO_2 films from sol–gel nanopowders

Both un-doped and Pd-doped sol–gel films have been obtained by the dipping procedure, using glass substrates (microscopic slides) by embedding the prepared TiO_2 sol–gel nanopowders (un-doped and Pd-doped) in the TiO_2 matrix, after the aging of the sol. A constant withdrawal speed of 5 cm min^{-1} has been used. The quantity of nanopowder related to the TiO_2 matrix was in all cases of 5 mass%. Figure 1 presents the scheme of the sol–gel coatings preparation.

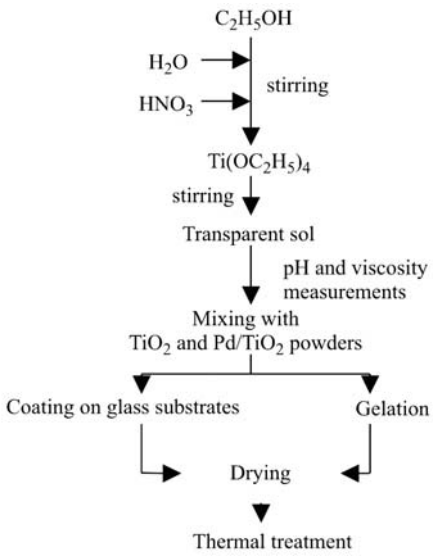

Fig. 1 The scheme of preparation of sol–gel TiO_2 based films from nanopowders

The obtained films have been dried at room temperature and then densified by thermal treatment. The thermal processing has been done at the same three temperatures: 300, 400 and 500°C, respectively, as in the case of powders and matrix, using in all cases the same heating rate of 1°C min^{-1}.

Methods of characterization

The thermal and crystallization behavior of the prepared samples were followed by thermal analysis, us-

ing a Mettler Toledo Star System TGA/SDTA851/LF 1600°C apparatus.

The structural evolution was studied by:

- XRD analysis with a Shimadzu XRD 6000 diffractometer, using Ni-filtered CuK_α radiation (λ=1.5418 Å) with a scan step of 0.02° and a counting time of 1 s/step, for diffraction angles 2θ ranged between 20 and 80°;
- IR spectroscopy performed on a Carl Zeiss Jena Specord M-80 IR spectrophotometer with KBr pellets technique;
- TEM with Jeol 200CX equipment;
- AFM images with a Nomad microscope from Quesant, in the intermittent contact regime.

The XRD analysis supplied valuable information in the study of the influence of Pd on TiO_2 crystallization materials by means of lattice parameters, crystallite sizes and internal strains determinations.

Hydrophilicity measurements have also been performed in order to establish the hydrophilic properties of the films, which were connected with their structure, composition and surface morphology. Film hydrophilicity was studied from contact angle (CA) measurements between drop volumes of 500 nL of deionized water and the film surface. CA measurements were performed at room temperature (25°C) under 65% environment humidity conditions. Details on the experimental device are presented elsewhere [17, 20]. Photoactivation was done by irradiating the samples with filtered UV light (100 mW cm^{-2}, photon energy: 3.18–3.65 eV) from a high-pressure mercury lamp. The CA angle *vs*. the UV irradiation dose was monitored until the saturation of the angle was reached. Then CA's were measured during the back-reaction regime, with UV irradiation removed, every 8 h, in eight time steps.

Results and discussion

Thermal analysis

The thermal behaviour of the gel of TiO_2 matrix-M (obtained from gelation of TiO_2 sol used from films preparation) and of TiO_2 and Pd-doped TiO_2 nanopowders are presented in Figs 2–4.

In Fig. 2, DTA curve shows an intense endothermic effect at 105°C, due to adsorbed water and alcohol removal and a slight one at 325°C due to the decomposition of the organic matter, both associated with mass loss (21.44% total mass loss) on TG curve. The presence of two maxima, at 273 and 320°C, on the DTG curve evidences that the decomposition takes place in two steps. The exothermic effect at 524°C on DTA curve can be assigned to the crystallization of TiO_2 rutile.

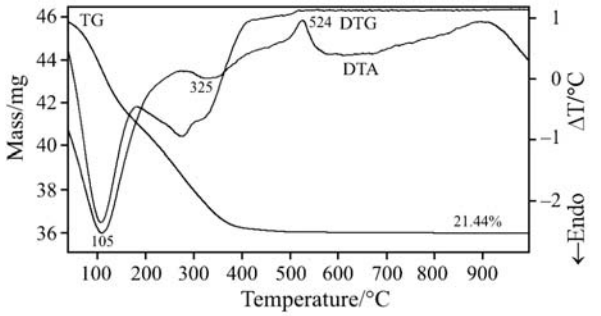

Fig. 2 Thermal behaviour of the gel of TiO_2 matrix (TiO_2-M)

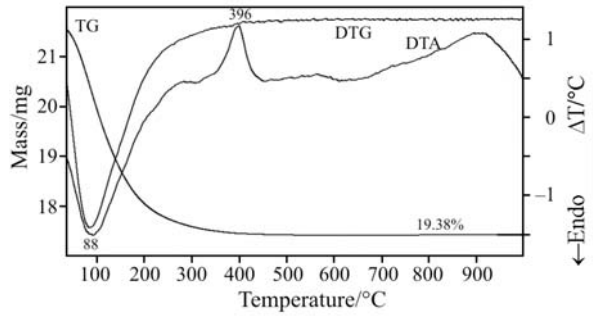

Fig. 3 Thermal behaviour of the TiO_2 nanopowder (TiO_2-P)

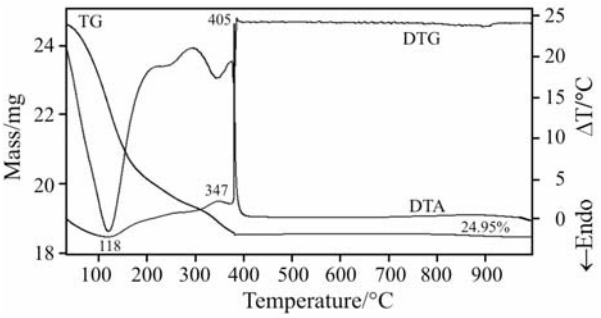

Fig. 4 Thermal behaviour of the Pd-doped TiO_2 nanopowder (TiO_2–1% Pd)

Unlike the TiO_2 matrix case, for the TiO_2 nanopowder (Fig. 3), TG and DTG curves show a continuous mass loss until 450°C (19.38%). An endothermic effect at 88°C on DTA curve is visible. The TiO_2 anatase crystallization effect can be observed at 396°C.

In Fig. 4, the same low temperature endothermic effect at 118°C on DTA curve, assigned to water and alcohol removal, associated with significant mass loss on TG curve can be observed. The total mass loss was of 24.95%. In this case the decomposition occurs in three steps with maxima at 245, 343 and 379°C. The last one overlaps with the sharp exothermic effect at 405°C due to the crystallization of TiO_2 anatase.

XRD results

The amorphous character of the thermally treated films was confirmed by XRD analysis. This is due to

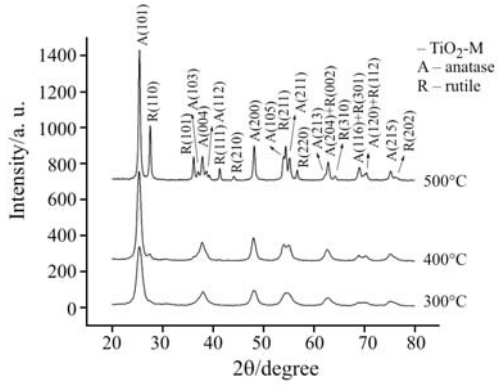

Fig. 5 XRD patterns of TiO_2 matrix (TiO_2-M) thermally treated at 300, 400 and 500°C/1 h

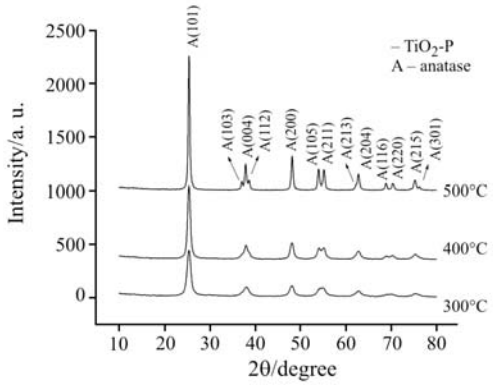

Fig. 6 XRD patterns of TiO_2 nanopowders (TiO_2-P) thermally treated at 300, 400 and 500°C/1 h

their small thickness (~500 Å), so that the phase composition was established for unsupported gels.

Structural evolution with temperature of the TiO_2 matrix and of the TiO_2 and Pd-doped TiO_2 nanopowders is presented by XRD patterns in Figs 5–7. XRD results are presented also in Table 1: the identified phases, the lattice constants and some microstructural factors were calculated from the computerized analysis of the XRD spectra.

For the un-doped and Pd-doped TiO_2 nanopowders only the presence of anatase was noticed, no

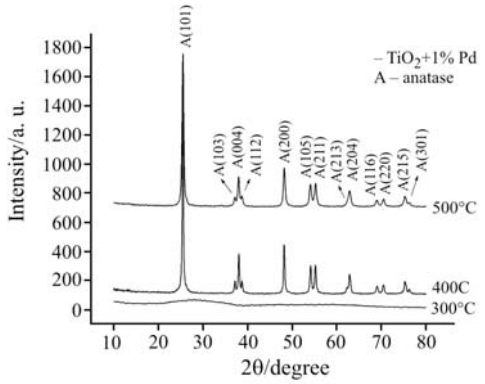

Fig. 7 XRD patterns of Pd-doped TiO_2 nanopowders (TiO_2–1% Pd) thermally treated at 300, 400 and 500°C/1 h

matter of temperature value. For TiO_2 matrix, a beginning of rutile crystallization, at detection limit of diffractometer (5%), was observed at 400°C.

In the case of Pd-doped TiO_2 sample, palladium decreases the crystallite size of anatase and increases the internal strains of the material, confirming the fact that Pd is inside of the TiO_2 network.

IR spectroscopy

IR spectra of TiO_2 matrix gel and of un-doped and Pd-doped TiO_2 nanopowders thermally treated (300–500°C) show the following vibration bands: 3440 cm^{-1} (ν_{OH}), 1640 cm^{-1} (δ_{HOH}), 670 cm^{-1} (ν_{Ti-O} of isolated tetrahedral TiO_4), 540 cm^{-1} (ν_{Ti-O} of condensed octahedral TiO_6) and 360 cm^{-1} (ν_{Ti-O} of isolated octahedra TiO_6) in agreement with literature data [21].

TEM measurements

For powders

TEM and SAED images of un-doped and Pd-doped TiO_2 powders are presented in Figs 8 and 9.

Table 1 Microstructural factors calculated from the computerized profile analysis of the XRD spectra

Sample	Phase	Microstructural factors				
		a/Å	*c*/Å	*V*/Å^3	*D*/Å	10^3S
TiO_2-M-300	anatase	3.7770(12)	9.4561(42)	134.90(14)	135(11)	3.61(45)
TiO_2-M-500	anatase	3.7756(16)	9.4740(57)	135.05(19)	453(48)	0.57(19)
	rutile	4.5886(38)	2.9561(30)	62.24(17)	685(148)	1.10(32)
TiO_2-P-300	anatase	3.7752(45)	9.4973(164)	135.36(56)	79(14)	9.9(1.5)
TiO_2-P-500	anatase	3.7750(19)	9.4828(68)	135.14(23)	346(8)	0.24(4)
TiO_2+1% Pd-300	amorphous	–	–	–	–	–
TiO_2+1% Pd-500	anatase	3.7725(17)	9.4533(62)	134.54(21)	351(8)	0.84(4)
TiO_2 standard	anatase (JCPDS 21-1272)	3.7852	9.5139	–	–	–
	rutile (JCPDS 21-1276)	4.5933	2.9592	–	–	–

a, *c* – lattice parameters; *V* – unit cell volume; *D* – crystallite size; *S* – internal strain

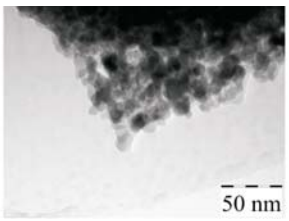

Fig. 8 TEM image of TiO_2 powder (TiO_2-P) thermally treated at 400°C

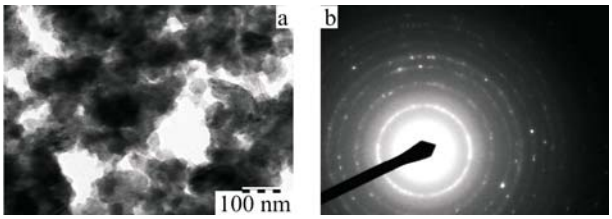

Fig. 9 a – TEM and b – SAED images of Pd-doped TiO_2 (TiO_2–1% Pd) thermally treated at 400°C

The TEM images of TiO_2 nanopowders evidence the presence of spheroidal TiO_2 nanocrystallites jointed in aggregates of 300–800 nm. The Pd-doped TiO_2 nanopowder presents anatase crystallites of 20–50 nm with a lot of internal defects.

For films

Figures 10 and 11 present the TEM micrographs of the TiO_2 films obtained from the sol matrix after the thermal processing.

As it can be seen, the prepared TiO_2 films are amorphous and their morphology evidences a nanometric porosity. The increase of temperature of the thermal treatment from 400 to 500°C determined the beginning of the crystallization and led to almost double sizes of pores.

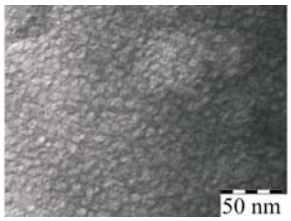

Fig. 10 TiO_2 film obtained from the sol matrix (M), thermally treated at 400°C

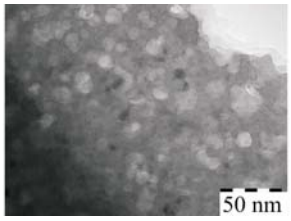

Fig. 11 TiO_2 film obtained from the sol matrix (M), thermally treated at 500°C

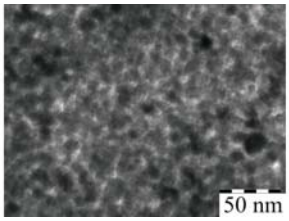

Fig. 12 TiO_2 film obtained from nanopowder (MT), thermally treated at 400°C

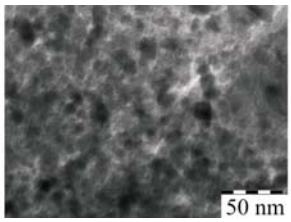

Fig. 13 TiO_2 film obtained from nanopowder (MT), thermally treated at 500°C

The TEM results referring to the pure TiO_2 films obtained from nanopowders (MT) are shown in Figs 12 and 13. The presented micrographs correspond also to the thermally treated samples.

The thermally treated (MT) TiO_2 films are crystallized at both temperatures of thermal processing, the sizes of crystallites increasing from a medium value of 10 nm (corresponding to 400°C) to 15 nm (at 500°C).

The TEM micrographs corresponding to the Pd-doped TiO_2 films (MTP) obtained from nanopowders and thermally treated at the same temperatures are presented in Figs 14 and 15.

As in the case of TiO_2 films obtained from the sol matrix, a beginning of crystallization can be observed at 500°C, compared to 400°C, when the film is amorphous.

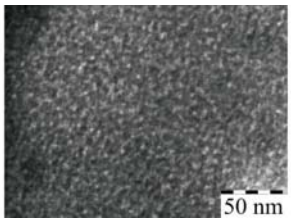

Fig. 14 Pd-doped TiO_2 film obtained from nanopowder (MTP), thermally treated at 400°C

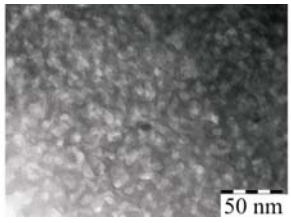

Fig. 15 Pd-doped TiO_2 film obtained from nanopowder (MTP), thermally treated at 500°C

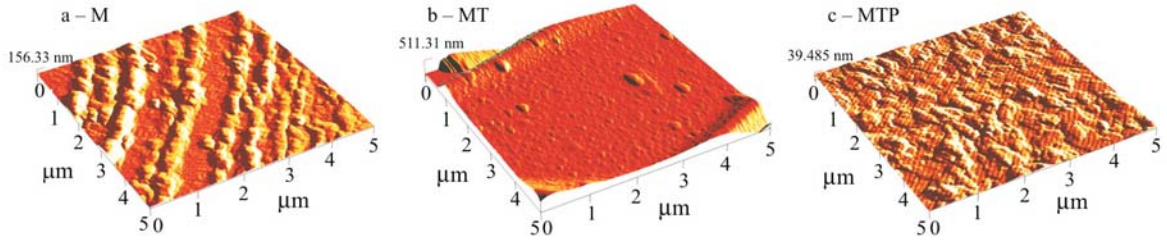

Fig. 16 AFM images of TiO_2 films thermally treated at 500°C, measured over an 5×5 µm area; Root–Mean–Square (RMS) deviation (roughness): 19.87; 57.1 and 4.97 nm, respectively. The *z*-scales marked in the left corner is depending on the largest height of depth measured on the selected area and is sensible different for each sample. In MT sample a deep crack could be observed hidding other profile details and conducting to the highest roughness

AFM measurements

AFM images of all prepared TiO_2 films (M, MT, MTP), thermally treated at 500°C are presented in Figs 16a–c. The un-doped TiO_2 films (MT) present the greatest value of RMS.

Test of hydrophilicity

Figure 17 indicates that the CA values range between 25 and 72° for the non-irradiated samples. Knowing that the super-hydrophilicity of a surface is indicated by CA values below 10° [22], we may consider that all the studied films become super-hydrophilic by UV irradiation, especially un-doped TiO_2 films obtained from nanopowders – MT films.

Also, these samples have the lowest initial CA values, which indicate that they are rougher than the others [20, 23]. For hydrophilic cases, CA<90°, the surface roughness has as effect the amplification of the wetting, as shown by the Wenzel model [24]. A rougher surface is a more open surface and it features low CA values due to its surface tension effects [24].

For all the other samples (M and MTP) it can be observed a sharp decrease of the contact angle towards values lower than 10°, for UV doses ranging between 5 and 15 J cm^{-2}.

After irradiation, by keeping the samples in darkness, the CA values increase for all the samples,

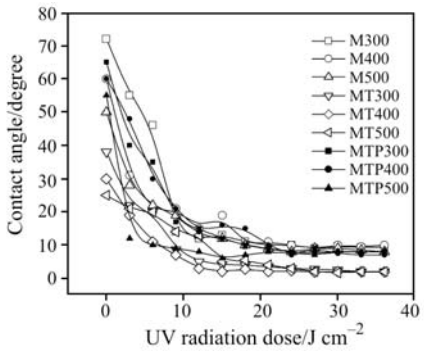

Fig. 17 Contact angle as a function of the UV irradiation dose for the studied titanium oxide films

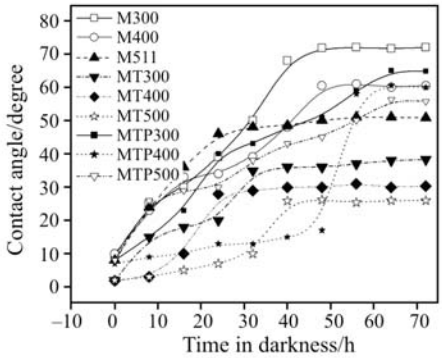

Fig. 18 Contact angle as a function of time measured under surface deactivation conditions

reaching the initial values in different time intervals as a function of films structure (Fig. 18).

There is a slowly recovery of the initial CA values for the MTP samples, as well as for the M samples, an exception being made for the MTP400 sample, for which the CA maintains its low values for nearly 50 h. For the MT samples recovery times of 20–30 h are observed

Anatase phase is known to be the most active phase in the photocatalysis process [22]. Here, all the samples are mainly anatase, which justify their good hydrophilic properties.

Conclusions

Un-doped and Pd-doped TiO_2 sol–gel nanopowders and the corresponding films coated on glass substrates prepared by embedding of these nanopowders in vitreous TiO_2 matrices were performed.

The thermal analysis and X-ray diffraction point out the differences in the crystallization behaviour between TiO_2 matrix and un-doped and Pd-doped TiO_2 nanopowders.

The influence of the dopant and of the thermal treatment on the films structure was established. Palladium decreases the crystallite size of anatase and in-

creases the internal strains of the material, confirming the fact that Pd is inside the TiO_2 network.

The hydrophilic properties of the films were connected with their structure, composition and surface morphology. All the studied films become super-hydrophilic by UV irradiation, especially un-doped TiO_2 films obtained from nanopowders; this is sustained by a greater crystallization tendency and the greatest RMS (roughness) values for the last ones.

Acknowledgements

This work was supported partially by the National Research Program CEEX, grants No. 642/2005-2008, 6113/2005-2008 and 103(12752)/2006-2008.

References

1 M. R. Hoffmann, S. T. Martin, W. Choi and D. W. Bahnemann, Chem. Rev., 95 (1995) 69.
2 J. M. Herrmann, Topics Catalysis, 34 (2005) 49.
3 D. F. Ollis and H. Al-Ekabi, Eds, Photocatalytic Purification and Treatment of Water and Air, Elsevier, Amsterdam 1993.
4 L. Zang, W. Macyk, C. Lange, W. Maier, C. Antonius, D. Meissner and H. Kisch, Chem. Eur. J., 6 (2000) 379.
5 R. Wang, K. Hashimoto, A. Fujishima, M. Chikuni, E. Kojima, A. Kitamura, M. Shimohigoshi and T. Watanabe, Adv. Mater., 10 (1999) 135.
6 M. Miyauchi, A. Nakajima, T. Watanabe and K. Hashimoto, Chem. Mater., 14 (2002) 2812.
7 J. Tang, H. Quan and J. Ye, Chem. Mater., 19 (2007) 116.
8 K. Zhang, W. Xu, X. Li, S. Zheng and G. Xu, Central Eur. J. Chem., 4 (2006) 234.
9 R. Campostrini, M. Ischia and L. Palmisano, J. Therm. Anal. Cal., 71 (2003) 997.
10 R. Campostrini, M. Ischia and L. Palmisano, J. Therm. Anal. Cal., 71 (2003) 1011.
11 R. Campostrini, M. Ischia and L. Palmisano, J. Therm. Anal. Cal., 75 (2004) 13.
12 R. Campostrini, M. Ischia and L. Palmisano, J. Therm. Anal. Cal., 75 (2004) 25.
13 T. Nishide, T. Tanaka and T. Yabe, J. Therm. Anal. Cal., OnlineFirst, DOI: 10.1007/s10973-007-7791-7.
14 I. Oja Açik, J. Madarász, M. Krunks, K. Tőnsuaadu, D. Janke, G. Pokol and L. Niinistö, J. Therm. Anal. Cal., 88 (2007) 557.
15 K. T. Ranjit, T. K. Varadarajan and B.Viswanathan, J. Photochem. Photobiol. A Chemistry, 96A (1996) 181.
16 S. Yuan, Q. Sheng, J. Zhang, F. Chen, M. Anpo and W. Dai, Catal. Lett., 107 (2006) 19.
17 D. Crişan, N. Drăgan, M. Crişan, M. Răileanu, A. Brăileanu, M. Gartner, M. Anastasescu, M. Zaharescu, A. Ianculescu, D. Mardare, D. Luca and V. E. Marinescu, XI International Conference on the Physics of Non-Crystalline Solids, Rhodes, Greece, 29.10-2.11 (2006), submitted to J. Phys. Chem. Solids.
18 M. Keshmiri, M. Mohseni and T. Troczynski, Appl. Catal. B: Environmental, 53 (2004) 209.
19 M. Crişan, A. Brăileanu, M. Răileanu, D. Crişan, V. S. Teodorescu, R. Bîrjega, V. E. Marinescu, J. Madarász and G. Pokol, J. Therm. Anal. Cal., 88 (2007) 171.
20 D. Luca, D. Mardare, F. Iacomi and C. M. Teodorescu, Appl. Surf. Sci., 252 (2006) 6122.
21 M. Crişan, A. Jitianu, M. Zaharescu, F. Mizukami and S. Niwa, J. Dispersion Sci. Technol., 24 (2003) 129.
22 A. Fujishima, T. Rao and D. Tryk, Photochem. Photobiol. C: Photochem. Rev., 1 (2000) 1.
23 D. Mardare, F. Iacomi and D. Luca, Thin Solid Films, 515 (2007) 6474.
24 R. N. Wenzel, J. Phys. Colloid. Chem., 53 (1949) 1466.

DOI: 10.1007/s10973-007-8720-5